DOI: 10.1007/s41230-016-5114-y

Fabrication, magnetostriction properties and applications of Tb-Dy-Fe alloys: a review

Nai-juan Wang [1], *Yuan Liu [1,2], Hua-wei Zhang [1,2], Xiang Chen [1,2], and Yan-xiang Li[1,2]

1. School of Materials Science and Engineering, Tsinghua University, Beijing 100084, China;

2. Key Laboratory for Advanced Materials Processing Technology (Ministry of Education), Beijing 100084, China

Abstract: As an excellent giant-magnetostrictive material, Tb-Dy-Fe alloys (based on $Tb_{0.27-0.30}Dy_{0.73-0.70}Fe_{1.9-2}$ Laves compound) can be applied in many engineering fields, such as sonar transducer systems, sensors, and micro-actuators. However, the cost of the rare earth elements Tb and Dy is too high to be widely applied for the materials. Nowadays, there are two different ways to substitute for these alloying elements. One is to partially replace Tb or Dy by cheaper rare earth elements, such as Pr, Nd, Sm and Ho; and the other is to use non-rare earth elements, such as Co, Al, Mn, Si, Ce, B, Be and C, to substitute Fe to form single $MgCu_2$-type Laves phase and a certain amount of Re-rich phase, which can reduce the brittleness and improve the corrosion resistance of the alloy. This paper systemically introduces the development, the fabrication methods and the corresponding preferred growth directions of Tb-Dy-Fe alloys. In addition, the effects of alloying elements and heat treatment on magnetostrictive and mechanical properties of Tb-Dy-Fe alloys are also reviewed, respectively. Finally, some possible applications of Tb-Dy-Fe alloys are presented.

Key words: magnetostriction; Tb-Dy-Fe alloy; fabrication method; applications

CLC numbers: TG143.9 **Document code:** A **Article ID:** 1672-6421(2016)02-075-10

1 Introduction

The cubic Laves phase RFe_2 compounds (R=Sm, Tb and Dy) with cubic $MgCu_2$-type structure have giant room temperature magnetostriction constants in excess of 2,000 ppm [1-4]. However, they also possess huge magnetocrystalline anisotropies [5], which needs large magnetic field in practical application. Considering that the sign of these magnetocrystalline anisotropy constants differs at room temperature, for example, $K_1 = +2.1\times10^7$ erg·cm^{-3} for $DyFe_2$ and $K_1 = -7.6\times10^7$ erg·cm^{-3} for $TbFe_2$ [6, 7], Clark et al. [8] suggested that the anisotropy of $TbFe_2$ could be lowered by introducing $DyFe_2$ compound for the anisotropy compensation. On this basis, they tailored the ternary Tb_{1-x}-Dy_x-Fe_{2-y} alloy to minimize the anisotropy yet maintaining the large magnetostriction. The optimal compositions occur near $0.7<x<0.73$ and $0<y<0.2$ [9, 10]. Tb-Dy-Fe alloys with the optimal composition are evenly marked with Terfenol-D which possesses a lower magnetocrystalline anisotropy constant ($K_1 = -0.06\times10^7$ erg·cm^{-3}), while maintaining a higher room temperature magnetostriction constant (λ_{111}=1,500–2,000 ppm) in its single crystal state [11-14]. This discovery yields a potential future for applications of giant magnetostrictive materials (GMM).

In the past four decades, many studies have been conducted during the development of Tb-Dy-Fe alloys with a large magnetostrictive but a small magnetic anisotropy and a low cost. Much work has been focused on increasing the ratio of magnetostriction to magnetocrystalline anisotropy through substituting other rare earth elements for Tb, Dy or transition metal elements for Fe. For example, some researchers proposed to replace Tb or Dy by Pr [15], Nd [16] and Ho [17], and to substitute Co [18], Al [19], Mn [19], Si [20], Zr [21] and Ce [22] for Fe, respectively. Beside alloy composition, the magnetostriction of the material can also be controlled by the grain orientation which is involved with the different easy magnetization directions (EMD) formed by different fabrication methods [23, 24]. Bridgman method [25-29], floating zone method [30-32] and Czochralski method [33-35] were used for preparing a single crystal grain orientation or twins, respectively. Moreover, heat treatment was also employed to improve comprehensive performances of the alloy by Hu Yong et al. [36] and Wei Wu et al. [37].

***Yuan Liu**

Male, born in 1974, Ph.D, Associate Professor. His research mainly focuses on the fabrication and application of porous metals, alloy solidification foundation and process and advanced metallic materials.

E-mail: yuanliu@tsinghua.edu.cn.

Received: 2015-11-09; Accepted: 2016-01-20

The fabrication methods for Tb-Dy-Fe alloys and the corresponding preferred growth direction are introduced in this paper. Moreover, effects of some alloying elements and heat treatment on magnetostrictive and mechanical properties of Tb-Dy-Fe alloys are reviewed, respectively. Finally, some possible applications of Tb-Dy-Fe alloys are presented.

2 Fabrication methods

Tb-Dy-Fe alloys with a single crystal or crystal orientation have good magnetostrictive properties [38]. To obtain this kind of crystal, directional solidification technology mainly including Bridgman method, floating zone method and Czochralski method are used for preparing the single crystal grain orientation or twins, respectively. In the following, these three methods will be introduced in detail.

2.1 Bridgman method

Bridgman method is named after P. W. Bridgman who is the first one using this method to grow a series of metal single crystals [25]. A typical Bridgman system is shown in Fig. 1(a). The movement of the crucible is controlled by a dropping motor. A longitudinal temperature profile is established at the center of the furnace with a specific temperature gradient near the melting point of the material, as shown in Fig. 1(b). The hole in the lid should be small and the lid should fit well with the furnace body to prevent thermal disturbance. The solidification interface moves up slowly along with the crucible which is cooled from one end to another.

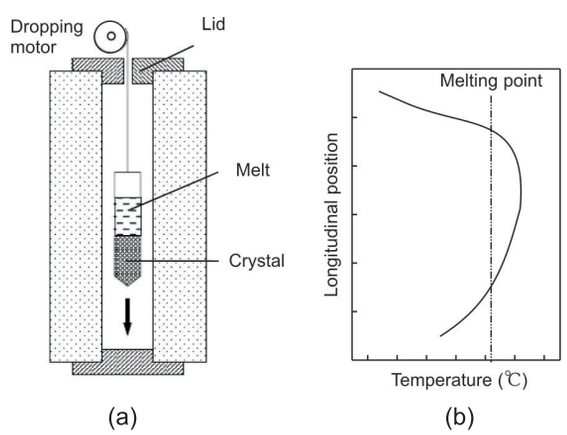

Fig. 1: A typical Bridgman system: (a) schematic diagram of furnace; (b) longitudinal temperature profile at furnace center [28]

There can be a seed or no seed for the crystal growth based on the Bridgman method. Given the orientation of seed crystal is <111>, when the movement velocity of induction coil is less than the alloy critical solidification rate, the alloy will grow along with the <111> axis without preferred orientation. However, it is harmful for the magnetostrive property due to the formation of RFe_3. When the induction coil movement velocity is faster than the alloy critical solidification rate, it is easy to form dendrites or cellular crystal with easy magnetization direction (EMD) <112> [26, 27]. There is little RFe_3 precipitates in this process. But rare earth is easy to burn in this way, and it is difficult to reach a high temperature gradient which has an adverse impact on the solidification structure. In addition, the Bridgman method has limitations and potential issues such as crucible contamination and constraint [29] as well as axial macrosegregation when the pre-alloyed ingots are used [23].

2.2 Floating zone method

The floating zone method is to grow crucible contamination-free crystal in such a process that the contamination of the melt and the restriction on the melting temperature of the grown crystal by the crucible material can be avoided [30, 38]. Figure 2(a) exhibits the schematic diagram of floating-zone crystal growth model.

The induction coil moves from one end to another, which leads to the melting and solidification of alloys alternately. Dendrites or cellular crystals with easy magnetization direction (EMD) of <112> are prone to form in this way, as shown in Fig. 2(b)[31]. However, this method requires the relative moving speed of the induction coil to be consistent with the heating power, the width of the molten zone, the liquid phase temperature as well as the liquid surface tension, which makes it difficult for practical preparation. At present, the method is mainly used in the fabrication of small-sized specimens.

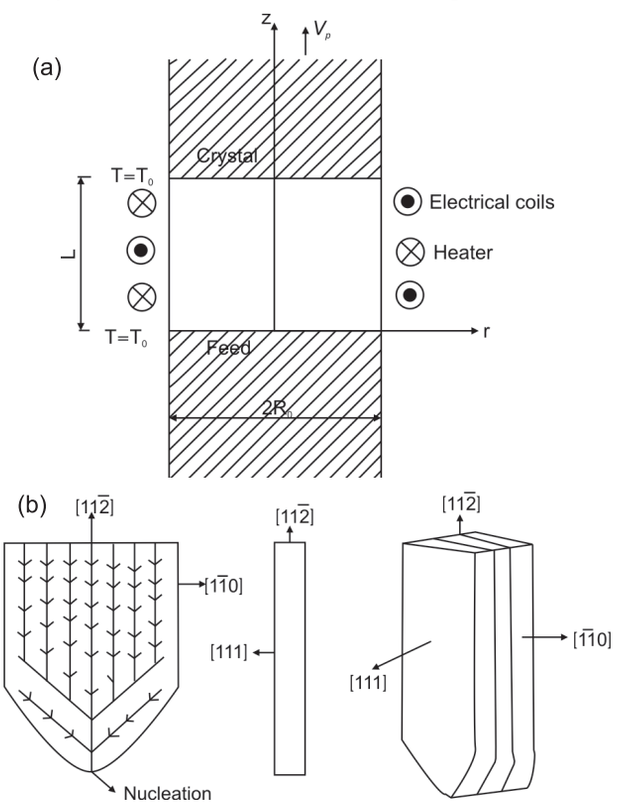

Fig.2 : (a) Schematic diagram of floating-zone crystal growth model [30]; (b) Dendritic platelets in $Tb_{0.27}Dy_{0.73}Fe_2$ [11]

2.3 Czochralski method

The Czochralski method [39] is a viable one-step route for preparing grain aligned rods of Tb-Dy-Fe alloys [33]. The schematic diagram of the process is shown in Fig. 3. The

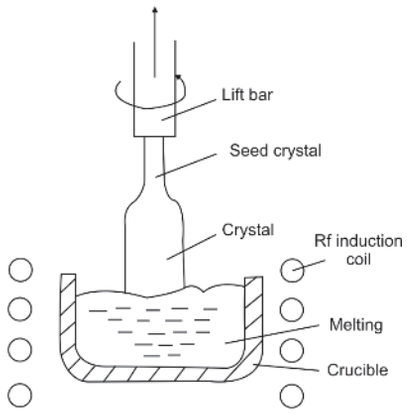

Fig.3 : Schematic diagram of $Tb_{0.3}Dy_{0.7}Fe_2$ produced by Czochralski method [38]

method is mainly composed of fixing a small grain (seed) to the rotatable tungsten rod, then inserting it into the mother alloy melt, thereafter pulling the seed crystal at a certain rate. Based on the seed, melt grows up into a single crystal [38].

The Czochralski technique is a preferred process in many single crystal growth experiments due to its great controllability over growth rate and the possibility of seeding crystals [29]. However, the overall melting process of raw materials with high temperature gradient which leads to volatility of rare earth elements resulting in composition deviation. Moreover, the slow pulling rate is easy to cause the precipitation of RFe_3 phase and Widmanstatten structure, which can reduce the magnetostrictive properties. The magnetostrictive coefficient is various with different easy magnetization directions, as shown in Fig. 4. The preferred EMD of the single crystal fabricated by this method is <111>.

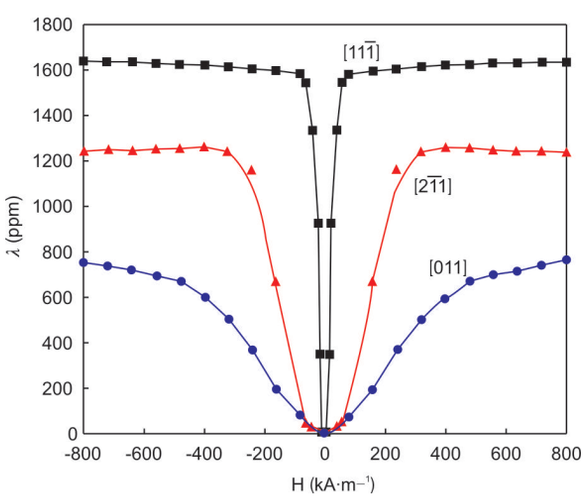

Fig. 4: Magnetic field dependences of magnetostriction for $Tb_{0.27}Dy_{0.73}Fe_2$ single crystal along the [111], [211] and [011] directions at demagnetized state [24]

From what has been discussed above, it can be found that it is difficult to obtain a bulk single crystal regardless of the methods for magnetostrictive material. Taking the crystal structure into consideration, preparing crystal along with the orientation direction can improve the magnetostriction properties.

3 Effects of substitute elements

Comparing with pure nickel and piezoelectric ceramic, Tb-Dy-Fe alloys possess many excellent characteristics such as large coupling coefficient, high energy density, high Curie temperature, large strain and better operation stability, and they have been widely studied and applied to ultrasonic transducer in recent years [40]. However, the high cost of Tb and Dy as well as certain brittleness of Tb-Dy-Fe alloys shortens the operating life-span and limits the large scale production [41]. In addition, the content of Fe element will also affect the characteristics of magnetostrictive materials. The content of RFe_3 can be increased with the increasing Fe content, whose magnetostrictive coefficient is quite lower than that of RFe_2, hence resulting in the reduction of the magnetostrictive coefficient [29]. Literatures show that it is feasible to stabilize the Laves phase, reduce brittleness, improve their corrosion resistance, and lower the cost, but without degrading magnetostrictive properties of the alloy by adding some alloying elements.

Nowadays, there are two different ways to substitute for alloy elements. One is to partially replace Tb or Dy by cheaper rare earth elements, such as Pr, Nd, Sm and Ho; the other one is to use non-rare earth elements, such as Co, Al, Mn, Si, Ce, B, Be and C, to substitute Fe and form single $MgCu_2$-type Laves phase and a certain amount of Re-rich phase, which can reduce the brittleness and improve the corrosion resistance of the alloy.

3.1 Substitute elements for Tb/Dy

3.1.1 Nd

$NdFe_2$ has a large theoretical spontaneous magnetostriction (the coefficient of λ_{111} is up to 2,000 ppm at 0 K). Moreover, the sign of anisotropy constant K1 for $NdFe_2$ is opposite to that of $TbFe_2$ which can reduce the magnetocrystalline anisotropy. Therefore, adding a certain amount of Nd into Tb-Dy-Fe can reduce the magnetocrystalline anisotropy of alloy instead of lowering the magnetostrictive coefficient. J. J. Liu et al [16] studied magnetic properties of $Tb_{0.4-x}Nd_xDy_{0.6}(Fe_{0.8}Co_{0.2})_{1.93}$. Results showed that there are optimal magnetic properties at x=0.05 and 10 KOe for external magnetic field (H). Figure 5 illustrates the magnetic-field and composition dependence of the magnetostriction of $Tb_{0.4-x}Nd_xDy_{0.6}(Fe_{0.8}Co_{0.2})_{1.93}$ alloys. The largest saturation magnetostriction coefficient can be up to 1,170 ppm.

In addition, H. Y. Yin et al. [42] found that the Laves phase compound of $Tb_{0.4}Dy_{0.5}Nd_{0.1}(Fe_{0.8}Co_{0.2})_{1.93}$ has a large spontaneous magnetostriction, and the coefficient of λ_{111} is about 1,640 ppm.

3.1.2 Ho

Ho has a smaller saturation magnetostriction than that of either Tb or Dy, thus the addition of Ho can reduce the magnetostriction of the alloy. However, the substitution of a small amount of Ho (<20%) for Tb or Dy resulted in a substantial decrease in hysteresis accompanied by only a small loss in magnetostriction [17, 43]. Such a tradeoff is very important for many device applications. M Wun-Fogle et al. [17] researched the magnetization and magnetostriction of dendritic

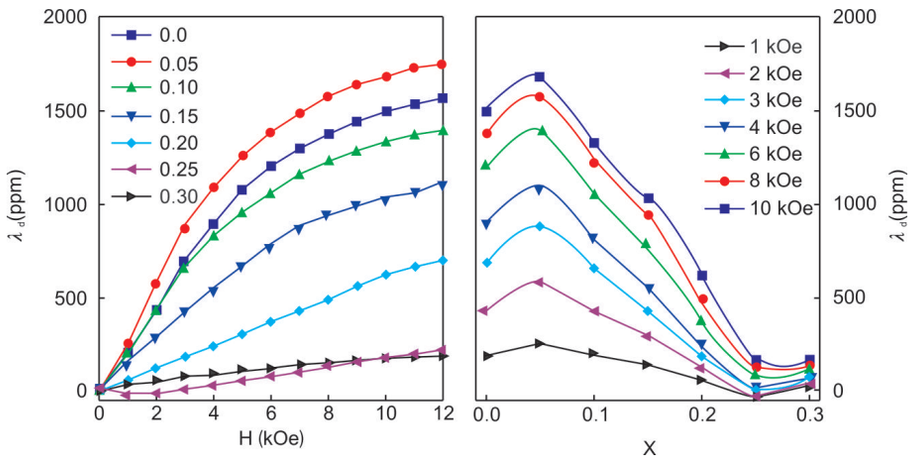

Fig. 5: (a) Magnetic-field dependence of magnetostriction λ_a (=$\lambda_{\parallel}$-$\lambda_{\perp}$) and (b) composition dependence of magnetostriction λ_a of $Tb_{0.4-x}NdxDy_{0.6}(Fe_{0.8}Co_{0.2})_{1.93}$ alloys [16]

[112] $Tb_xDy_yHo_{1-x-y}Fe_{1.95}$ rods under compressive stress. Adding Ho into the ternary alloy can clearly reduce the hysteresis, as shown in Fig. 6. Bowen Wang et al. [44] prepared and studied the $x(Tb_{0.15}Ho_{0.85}Fe_2)+(1-x)(Tb_{0.3}Dy_{0.7}Fe_2)$ alloys. It was found that the magnetostriction of alloys decreased with the increase of x. But the ratio ($\lambda///W_h$) of magnetostriction to hysteresis increases first and exhibits a peak when x=0.1, and then decreases with the increase of Ho content, as shown in Fig. 7. S.C. Busbridge et al. [45] manufactured $Tb_{0.20}Dy_{0.22}Ho_{0.58}Fe_2$ alloy, and tested the magnetostriction coefficient at different temperatures. Results claim that with the temperature decrease, the magnetostriction coefficient of the alloy significantly decreases at low magnetic field, whereas shows a tendency to rise at high magnetic field. This is mainly because the EMD transferred from <111> to <100> with the decrease of temperature.

3.1.3 Pr

Because of high magnetostriction of $PrFe_2$ (close to $5,600\times10^{-6}$) [46], it attracts much attention in the research field of magnetostictive materials. At the same time, the magnetocrystalline anisotropy constant of $PrFe_2$ is opposite to $TbFe_2$ [47], thus the addition of Pr can reduce the magnetocrystalline anisotropy constant of the alloy. Single-

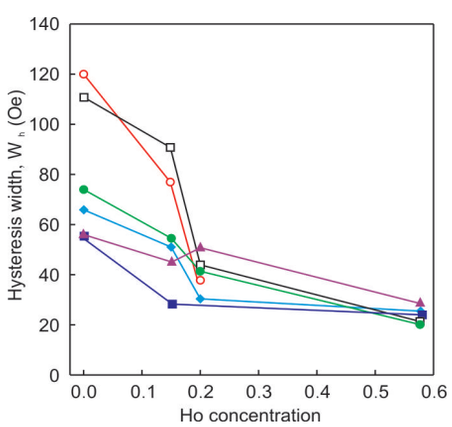

Fig. 6: Hysteresis width W_h vs Ho concentration for samples under applied stresses of -9.8 (filled square), -21.9 (filled triangle), -33.9 (filled diamond), -46.0 (filled circle), -58.1 (open square), and -70.1 MPa (open circle) [17]

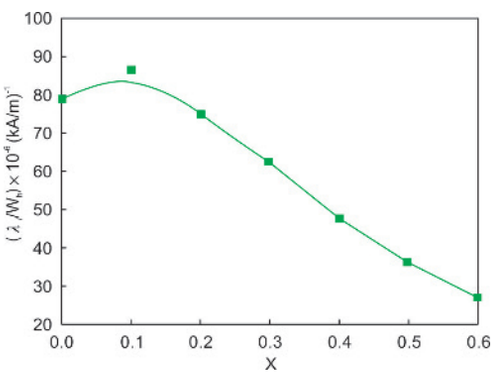

Fig. 7: Ratio ($\lambda///W_h$) of magnetostriction to hysteresis for $x(Tb_{0.15}Ho_{0.85}Fe_2)+(1-x)(Tb_{0.3}Dy_{0.7}Fe_2)$ alloys in different compositions at a magnetic field of 320 kA·m^{-1} [44]

ion model [48] demonstrates that the ideal radius ratio of Laves phase between rare earth ions and Fe ion is 1.225. However, the radius of Pr_3^+ is larger than that of the ideal rare earth ions, which deviates much from the ideal radius ratio [49]. Therefore, the addition amount of Pr should not exceed 20%, otherwise it is easy to form impurity phase [49]. Ren Zhi et al. [15] studied the structure and magnetostriction of $Pr_xTb_{0.2}Dy_{0.8-x}Fe_{1.85}C_{0.05}$ (x=0.1−0.4) alloys. The research shows that RFe_3 phase and rare earth phase appeared when $x\geqslant0.2$, which leads to the decrease of magnetostriction coefficient and Curie temperature. Figure 8 depicts the magnetostriction coefficient and Curie temperature of the $Pr_xTb_{0.2}Dy_{0.8-x}Fe_{1.85}C_{0.05}$ (x=0.1−0.4) alloy, and it can be seen that $Pr_{0.2}Tb_{0.2}Dy_{0.6}Fe_{1.85}C_{0.05}$ alloy shows good magnetostrictive properties. Adding B into TbDyPrFe alloys can restrain the formation of RFe_3, therefore it can increase the amount of Pr to 30%. W. J. Ren et al. [50] studied the $Tb_xDy_{0.7-x}Pr_{0.3}(Fe_{0.9}B_{0.1})_{1.93}$ alloy, and the result showed that $Tb_{0.25}Dy_{0.45}Pr_{0.3}(Fe_{0.9}B_{0.1})_{1.93}$ alloy possesses excellent magnetostrictive properties with $\lambda_{111}\approx1,850$ ppm. Moreover, W. J. Ren et al. [51, 52] investigated $Tb_{0.2}Dy_{0.82x}Pr_x(Fe_{0.9}B_{0.1})_{1.93}$ (0<x<0.7) alloys and found that $Tb_{0.2}Dy_{0.4}Pr_{0.4}(Fe_{0.9}B_{0.1})_{1.93}$ alloy with the single Laves phase has a large magnetostriction (λ_{111}=1,200 ppm) and a low anisotropy. This alloy may be a good candidate for magnetostriction applications.

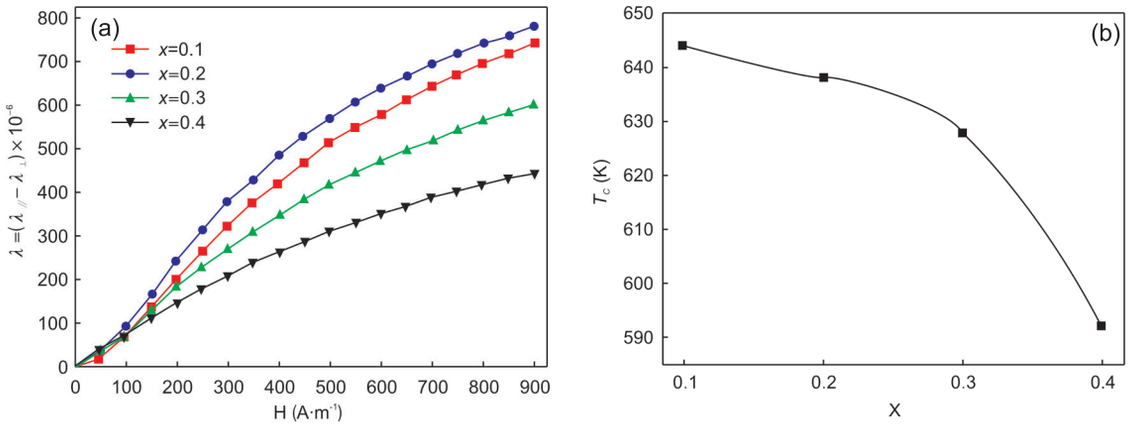

Fig. 8: Magnetostriction coefficient vs. magnetic field H (a) and Curie temperature vs. x (b) of alloy $Pr_xTb_{0.2}Dy_{0.8-x}Fe_{1.85}C_{0.05}$ (x=0.1–0.4) [15]

3.2 Substitute elements for Fe

3.2.1 Al /Mn

Under low magnetic field, the addition of a small amount of Al can lower the magnetocrystalline anisotropy of the material, but the magnetostrictive coefficient can be decreased with an increase in Al content. Meanwhile, Curie temperature will be reduced. In addition, Al is regarded as an ideal substituent for Fe to increase the resistivity and ductility [19]. Manganese is an effective substitution element to improve the magnetostrictive property of the Tb-Dy-Fe alloys. It is noted that the magnetostriction of Mn-containing compounds is larger than that of Mn-free compounds especially in the lower temperature region. And the addition of Mn can lower the anisotropy energy, and therefore, a low bias field for saturation magnetostriction is expected. This low bias magnetic field is very useful since it is sometimes decisive in the practical application [19].

3.2.2 Co

The addition of a small amount of Co can stabilize the Laves phase [16], but can reduce the magnetostriction coefficient of materials at the same time [18]. Replacing Fe by a small amount of Co can increase the alloy's Curie temperature T_C, but T_C will be deceased with the further increase of Co. Z. J. Guo et al. [18] studied the magnetostrictive properties of $(Tb_{0.7}Dy_{0.3})Pr_{0.3}(Fe_{1-x}Co_x)_{1.85}$, and the results are shown in the Fig. 9 and Fig. 10, respectively. With increasing Co content, the saturation magnetostriction coefficient decreases, but the Curie temperature obtains maximum value at x=0.3. As the Co content continues to increase, the Curie temperature tends to decline.

Z. B. Pan et al. [53] found that the Co element plays an opposite role in the resultant anisotropy as compared with Tb. The smallest anisotropy is obtained for the $Tb_{0.3}Dy_{0.6}Nd_{0.1}(Fe_{0.8}Co_{0.2})_{1.93}$ compound, which has good magneto-elastic properties, such as the large saturation magnetostriction λ_S(~930 ppm) and the high low-field magnetostriction λ_a(~670 ppm/3 kOe).

3.2.3 Si

Eddy current is formed easily in the process of Tb-Dy-Fe alloy in practical applications, which reduces the efficiency of the transducers. Studies have shown that the eddy current coefficient is inversely proportional to the electrical resistivity for magnetic material [20]. Thus, increasing electrical resistivity is a good means

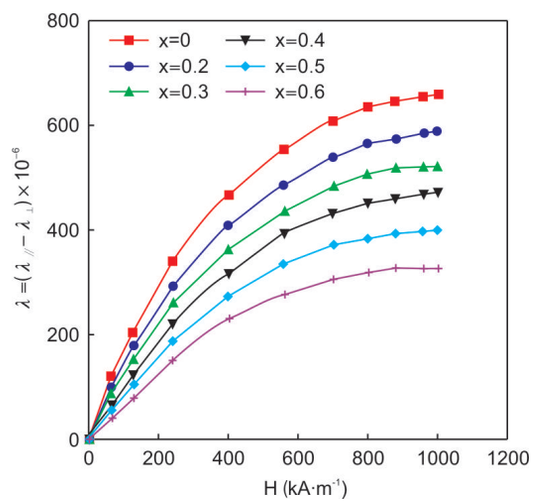

Fig. 9: Magnetic field dependence of room temperature magnetostriction λ of annealed polycrystalline $(Tb_{0.7}Dy_{0.3})Pr_{0.3}(Fe_{1-x}Co_x)_{1.85}$ alloys [18]

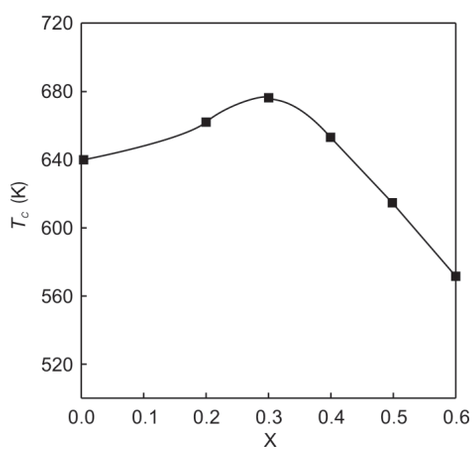

Fig. 10: Dependence of Curie temperature of $(Tb_{0.7}Dy_{0.3})Pr_{0.3}(Fe_{1-x}Co_x)_{1.85}$ alloys as a function of composition [18]

to reduce the resistivity of the alloy. Some researchers found that adding a certain amount of Si into Tb-Dy-Fe alloy can clearly improve the resistivity [20]. Silicon can be randomly dispersed into the alloy to become the conduction electron scattering center. With the increase of Si content, the number of conduction electrons

transferring into the localized 4f orbital of Tb or Dy is increased, but the number of remaining conduction electrons is decreased, which leads to the rise of resistivity. Lihong Xu et al [20] prepared the $Tb_{0.3}Dy_{0.7}(Fe_{1-x}Si_x)_{1.95}$ (x=0,0.025,0.1) alloys with orientation <110>, and studied the magnetostriction coefficient and resistivity along with the change of Si content. Results showed that when x increases to 0.025, the magnetostrictive coefficient drops slightly, but its resistivity increases significantly up to 100 mu Ω cm, as shown in Fig. 11 and Fig. 12, respectively.

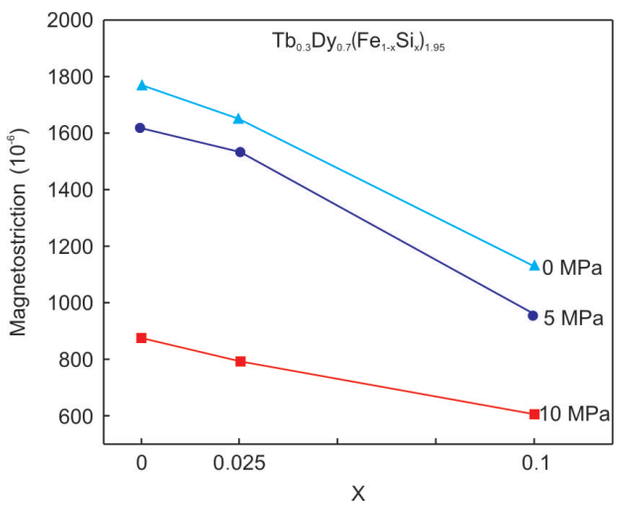

Fig. 11: Si content dependence of magnetostriction of<110> oriented $Tb_{0.3}Dy_{0.7}(Fe_{1-x}Si_x)_{1.95}$ (x=0, 0.025, 0.1) samples at room temperature [20]

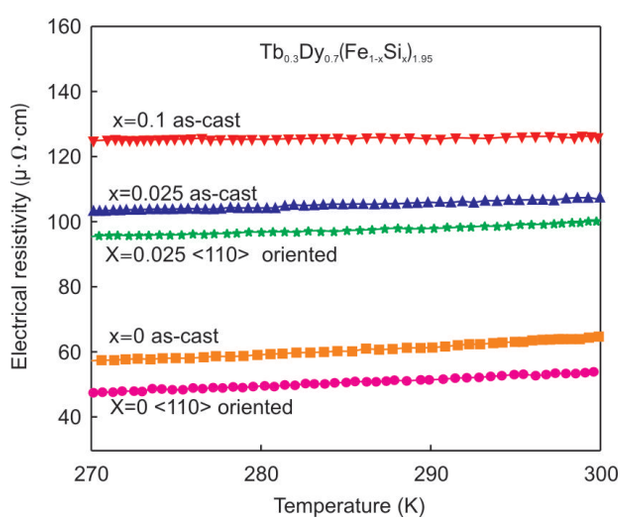

Fig. 12: Temperature dependence of electrical resistivity of $Tb_{0.3}Dy_{0.7}(Fe_{1-x}Si_x)_{1.95}$ (x=0,0.025, 0.1) in the temperature range from 250 to 300 K [20]

In addition, adding small amount of Si into alloy can improve the corrosion resistance. The reason is that the addition of Si improves the natural corrosion potential of the rare earth rich phase, which reduces the electrochemical potential difference between the rare earth rich phase and matrix phase. Lihong Xu et al. [54] studied the magnetic and corrosion resistance properties of $Tb_{0.3}Dy_{0.7}(Fe_{1-x}Si_x)_{1.95}$ (x=0, 0.025, 0.10) in 3.5% NaCl solution. Figure 13 illustrates the potentiodynamic anodic

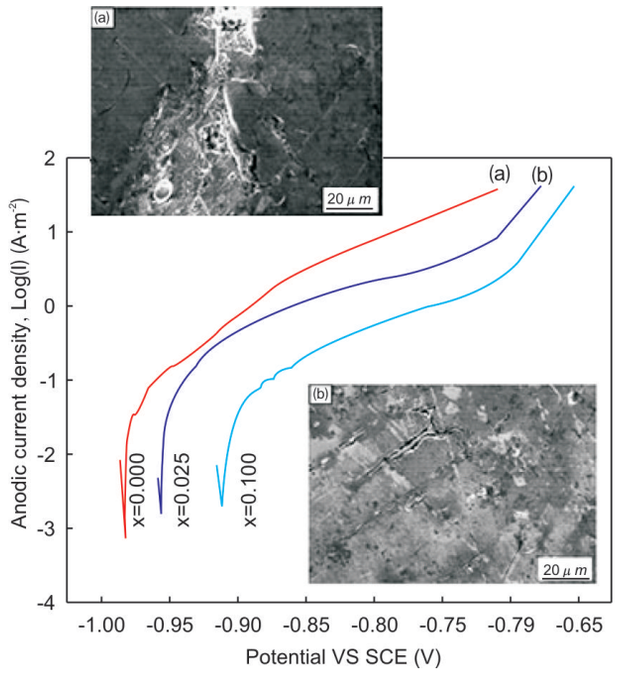

Fig. 13: Potentiodynamic anodic polarization curves of $Tb_{0.3}Dy_{0.7}(Fe_{1-x}Si_x)_{1.95}$ (x = 0, 0.025 and 0.1) in 3.5wt.% NaCl aqueous solution. SEM surface morphology after corrosion test of $Tb_{0.3}Dy_{0.7}Fe_{1.95}$ alloy (a), and $Tb_{0.3}Dy_{0.7}(Fe_{0.975}Si_{0.025})_{1.95}$ alloy (b) [54]

polarization curves of $Tb_{0.3}Dy_{0.7}(Fe_{1-x}Si_x)_{1.95}$ (x=0, 0.025 and 0.1) in 3.5wt.% NaCl aqueous solution, and the SEM surface morphology after corrosion test of $Tb_{0.3}Dy_{0.7}Fe_{1.95}$ alloy (a), and $Tb_{0.3}Dy_{0.7}(Fe_{0.975}Si_{0.025})_{1.95}$ alloy (b). The surface morphology after corrosion test indicates that the corrosion resistance of x=0.025 is better than that of the alloy without Si.

3.2.4 Zr

Li Xiaocheng et al. [21] replaced partial Fe of $Tb_{0.3}Dy_{0.7}Fe_{1.95}$ alloy by Zr. The addition of different amounts of Zr (x=0, 0.03, 0.06 and 0.09) has varying effects on alloy magnetostrictive properties. The addition of a small amount of Zr can effectively restrain the formation of harmful RFe_3 phase, which is good for the improvement of magnetostrictive properties. However, the precipitation of Zr rare earth rich phase is harmful to the magnetostriction enhancement when x=0.09, which has been shown in Fig. 14.

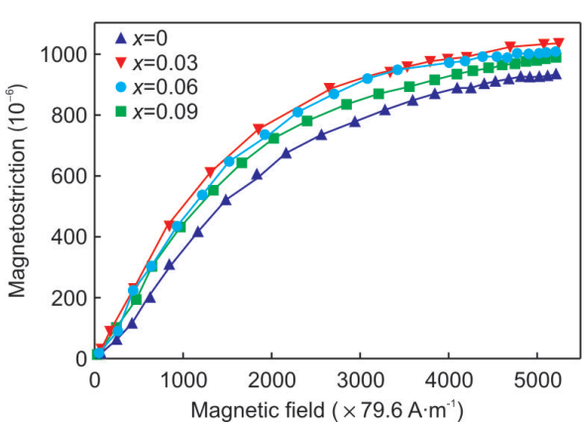

Fig. 14: Magnetostriction and magnetic field strength curves of alloy $Tb_{0.3}Dy_{0.7}Fe_{1.95-x}Zr_x$ (x=0.03, 0.06, 0.09) [21]

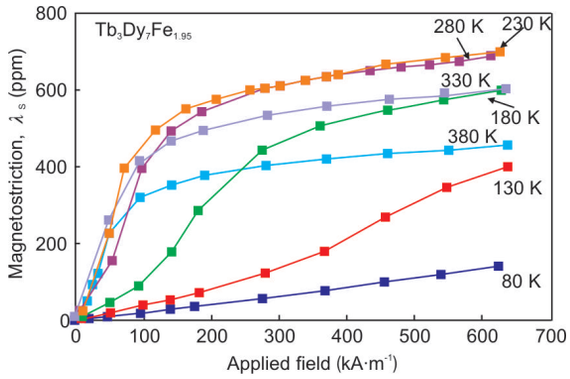

Fig. 15: Magnetostriction of $Tb_{0.3}Dy_{0.7}(Ce_zFe_{1-z})_{1.95}$ as a function of applied field and temperature as z=0.75 [22]

3.2.5 Ce

Colm Mac Mahon et al [22] investigated the magnetization and magnetoelastic properties of melt-spun ribbons of $Tb_{0.3}Dy_{0.7}(Ce_zFe_{1-z})_{1.95}$ ($0.025 \leqslant z \leqslant 0.2$). The ribbons exhibit a nanocrystalline structure which becomes more amorphous with increasing Ce content. Room temperature coercivities remain to be 80 $kA \cdot m^{-1}$, but low temperature coercivities increase with the Ce percentage. Saturation magnetostriction varies considerably with the addition of Ce, reaching a maximum of 850 ppm at 230 K, for $z = 0.075$ composition as shown in Fig. 15.

4 Heat treatment

The properties of Tb-Dy-Fe alloys are closely related to the material microstructure. After directional solidification, the Tb-Dy-Fe alloys are usually composed of RFe_2 phase and Re-rich phase [38]. The existence of the Re-rich phase can improve the toughness of the alloys [55]. Heat treatment can be used to optimize the morphology of the Re-earth phase, reduce defects, and lower inner stress of the alloys, so that the brittleness of material is improved [56]. According to the difference of heat treatment time and procedure, the heat treatment can be divided into one-step treatment and two-step treatment.

Hu Yong et al. [36] prepared <110> oriented $Tb_{0.3}Dy_{0.7}Fe_2$ alloy by the method of zone-melting directional solidification. Results show that the directional solidification Tb-Dy-Fe alloys annealed at 1,203 K for 2 h can achieve optimal performance with saturation magnetostriction of 1,226 ppm and compressive strength of 256 MPa. In addition, slow cooling rate can promote high magnetostrictive and mechanical properties. Chengbao Jiang et al [57] have successfully prepared <110> oriented rods of TbDyFe magnetostrictive alloys by zone melting unidirectional solidification. The homogenization annealing for 4 h and 48 h at 1,273 K have been conducted in a quartz cylinder under Ar atmosphere after pumping to 2×10^{-3} Pa. A satisfactory magnetostrictive property of $1{,}970 \times 10^{-6}$ was obtained under 15 MPa pre-stress after heat treatment for 4 h, but there was not further improvement for 48 h annealing.

Wei Wu et al [55] have also prepared <110> oriented rods of TbDyFe giant magnetostrictive alloy using zone melting directional solidification method. Two-step heat treatments were performed at 1,353 K for 2 h, followed by heating at 673, 773, 873, and 973 K for 4 h in Ar atmosphere and air cooling, respectively. Results showed that the alloy can get magnetostriction of 1,324 ppm and compressive strength of 585.16 MPa in a magnetic field of 80 $kA \cdot m^{-1}$ under 5 MPa pre-stress.

5 Applications

The rare earth giant magnetostrictive material (GMM) is an excellent new functional material. Comparing with pure nickel and piezoelectric ceramic, Tb-Dy-Fe alloys possess large coupling coefficient and high Curie temperature as well as higher magnetostriction coefficient [39, 40, 58], and have attracted much attention for applications in high power energy conversion devices [59-61]. For example, Tb-Dy-Fe alloys can be widely used in the design of a large-scale ultrasonic cleaning device for boat cleaning [62-67], device for high power ultrasonic spot welding (USW) [68-74], and device for therapeutic ultrasound (higher power ultrasound at lower frequencies) [75,76]. Moreover, Tb-Dy-Fe alloys also have a potential future in oil exploitation and pipeline transportation [77], and the recycling of waste energy [78-86], such as the emulsification and desulfurization of waste tires [87,88]. Figure 16 exhibits a large-scale ultrasonic cleaning system, and the schematic picture of a multi-transducer device for boat cleaning (20 kHz). Figure 17 shows the application and the component of the ultrasonic transducer in high-power ultrasonic oil production. Figure 18 shows the state of the pipeline before installation and six months after installation of the Tb-Dy-Fe ultrasonic transducer.

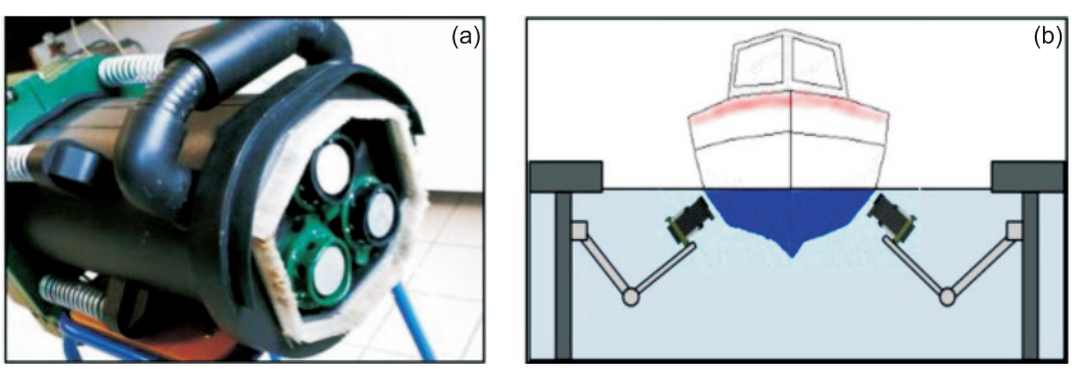

Fig. 16: Cleaning tool: (a) Photograph; (b) cleaning station with two devices [66]

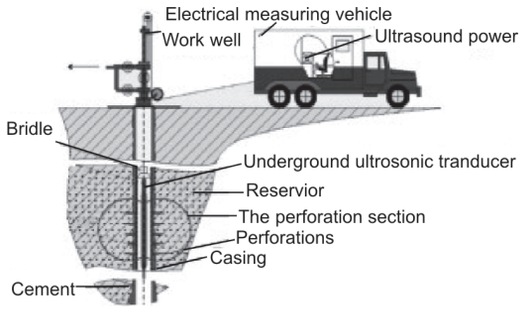

Fig. 17: Composition of CSYY60H10 high-power ultrasonic oil production [77]

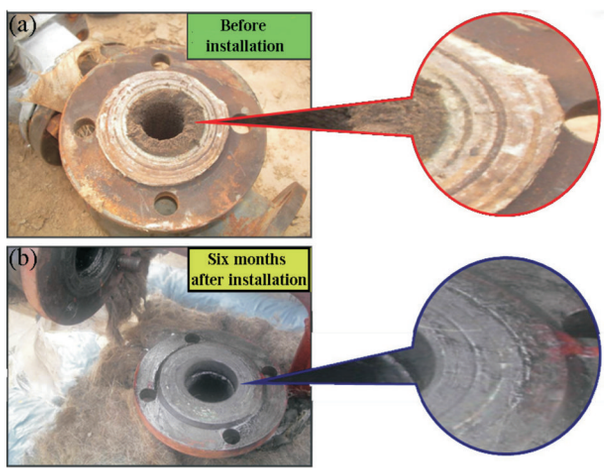

Fig. 18: State of pipeline (a) before installation and (b) six months after installing Tb-Dy-Fe ultrasonic transducer

6 Conclusion

Giant magnetostrictive material (GMM) is a strategic functional material in the 21st century. Recently, this kind of material showed a very broad application prospects in military and civilian dual-use high-tech areas. It has replaced the traditional magnetostrictive materials and has been widely used in advanced technologies, such as magnetomechanical transducers, actuators and adaptive vibration control systems. As an excellent GMM, Tb-Dy-Fe alloy possesses large magnetostriction strain, high energy conversion efficiency, and rapid response rate which have attracted much attention for applications in high power energy conversion devices. However, the cost of the rare earth element Tb and Dy is too high to be widely applied for the materials. Literatures show that it is feasible to enhance magnetostrictive properties of the alloy by adding some alloying elements. Nowadays, there are two different ways to substitute for alloy elements. One is to partially replace Tb or Dy by cheaper rare earth elements, such as Pr, Nd, Sm and Ho; the other one is using non-rare earth elements, such as Co, Al, Mn, Si, Ce, B, Be and C, to substitute Fe to form single $MgCu_2$-type Laves phase and a certain amount of Re-rich phase, which can reduce the brittleness and improve the corrosion resistance of the alloy.

As mentioned above, the properties of the Tb-Dy-Fe alloys play an important role in applications. Therefore, it is critical to develop new RFe_2 compound-based giant-magnetostrictive alloys with excellent properties and lower cost.

References

[1] Clark A E. Magnetic and magnetoelastic properties of highly magnetostrictive rare earth-iron laves phase compounds. American Institute of Physics Conference Series, 1974, 18: 1015–1029.

[2] Clark A E, Belson H S. Giant Room-Temperature Magnetostrictions in $TbFe_2$ and $DyFe_2$. Physical Review B, 1972, 5(9): 3642–3644.

[3] Tian Shi. Physical Properties of Materials. Beihang University Press, Beijing, China, 2004: 301. (in Chinese)

[4] Harsh D C and Manfred W. Non-Joulian magnetostriction. Nature, 2015, 521: 341–343.

[5] Liu X Y, Liu J J, Pan Z B, et al. Optimization on magnetic anisotropy and magnetostriction in $Tb_xHo_{0.8-x}Pr_{0.2}(Fe_{0.8}Co_{0.2})_{1.93}$ compounds. Journal of Magnetism and Magnetic Materials, 2015, 391: 60–64.

[6] Abbundi R, Clark A E. Anomalous thermal expansion and magnetostriction of single crystal $Tb_{0.27}Dy_{0.73}Fe_2$. IEEE Transactions on Magnetics, 1977, 1(5): 1519–1520.

[7] Jiles D C. The development of highly magnetostrictive rare earth-iron alloys. Journal of Physics D: Applied Physics, 1994, 27(1): 1–11.

[8] Clark A E. Magnetostrictive rare earth-Fe_2 compounds. Handbook of Ferromagnetic Materials, 1980, 1: 531–589.

[9] Verhoeven J D, Ostenson J E, Gibson E D. The effect of composition and magnetic heat treatment on the magnetostriction of $Tb_xDy_{1-x}Fe_y$ twinned single crystals. Journal of Applied Physics, 1989, 66(2): 772–779.

[10] Clark A E, Teter J P, McMasters O D. Magnetostriction "jumps" in twinned $Tb_{0.3}Dy_{0.7}Fe_{1.9}$. Journal of Applied Physics, 1988, 63(8): 3910–3912.

[11] Clark A E. Magnetostriction in twinned [112] crystal of $Tb_{0.27}Dy_{0.73}Fe_2$. IEEE Transaction on Magnetics, 1986, 22(5): 973–975.

[12] Jiles D C, Thoelke J B. Modelling of the combined effects of stress and anisotropy on the magnetostriction of $Tb_{0.3}Dy_{0.7}Fe_2$. IEEE Transactions on Magnetics, 1991, 27(6): 5352–5354.

[13] Clark A E, Belson H S, Strakna R E. Elastic properties of rare-earth-iron compounds. Journal of Applied Physics, 1973, 44(6): 2913–2914.

[14] Wang Bo-wen, Yan Rong-ge. Rare-earth Giant Magnetostrictive Materials, Application and Devices. Journal of Hebei University of Technology, 2004, 33(2): 16–22.

[15] Ren Zhi, Li Song-tao, Liu He-yan, et al. Structure and magnetostriction of $Pr_xTb_{0.2}Dy_{0.8-x}Fe_{1.85}C_{0.05}$ alloys. J Magn Mater Devices, 2013, 44(5): 6–7.

[16] Liu J J, Pan Z B, Liu X Y, et al. Large magnetostriction and direct experimental evidence for anisotropy compensation in $Tb_{0.4-x}Nd_xDy_{0.6}(Fe_{0.8}Co_{0.2})_{1.93}$ Laves compounds. Materials Letters, 2014(137): 274–276.

[17] Wun-Fogle M, Restorff J B, Clark A E, et al. Magnetization and magnetostriction of dendritic [112] $Tb_xDy_yHo_zFe_{1.95}$ (x+y+z=1) rods under compressive stress. Journal of Applied Physics, 1998, 83(11): 7279–7281.

[18] Guo Z J, Busbridge S C, Wang B W, et al. Structure and Magnetic and Magnetostrictive Properties of $(Tb_{0.7}Dy_{0.3})_{0.7}Pr_{0.3}(Fe_{1-x}Co_x)_{1.85}$($0 \leqslant x \leqslant 0.6$). IEEE Transactions on Magnetics, 2001, 37(4): 3025–3027.

[19] Du J, Wang J H, Tang C C, et al. Magnetostriction in twin-free single crystals $Tb_yDy_{1-y}Fe_2$ with the addition of aluminum or manganese. Applied Physics Letters, 1998, 72(4): 489–491.

[20] Lihong Xu, Chengbao Jiang, Huibin Xua. Magnetostriction and electrical resistivity of Si doped $Tb_{0.3}Dy_{0.7}Fe_{1.95}$ oriented crystals. Applied Physics Letters, 2006, 89(19): 1–3.

[21] Li Xiao-cheng, Ding Yu-tian, Hu Yong. Effects of Zr addition on the microstructure and megnetostriction of the as cast $Tb_{0.3}Dy_{0.7}Fe_{1.95}$ alloys. Journal of Functional Materials, 2011, 42(12): 2257–2260.
[22] Mahon C M, Jenner A G, Ahlers H. Magnetization and magnetostriction of melt-spun TbDyCeFe ribbons. IEEE Transactions on Magnetics, 2000, 36(5): 3214–3216.
[23] Park W J, Kim J C, Ye B J, et al. Macrosegregation in Bridgman growth of Terfenol-D and effects of annealing. Journal of Crystal Growth, 2000, 212(1): 283–290.
[24] Wang B W, Busbridge S C, Li Y X, et al. Magnetostriction and magnetization process of $Tb_{0.27}Dy_{0.73}Fe_2$ single crystal. Journal of Magnetism and Magnetic Materials, 2000, 218: 198–202.
[25] Bridgman P W. Certain Physical Properties of Single Crystals of Tungsten, Antimony, Bismuth, Tellurium, Cadmium, Zinc, and Tin. Proceedings of the American Academy of Arts and Sciences, 1925, 60(6): 305–383.
[26] Clark A E, Teter J P, Wun-Fogle M, et al. Magnetomechanical coupling in Bridgman-grown $Tb_{0.3}Dy_{0.7}Fe_{1.9}$ at high drive levels. Journal of Applied Physics, 1990, 67(9): 5007–5009.
[27] Verhoeven J D, Gibson E D, McMasters O D, et al. The growth of single crystal Terfenol-D crystals. Metallurgical Transactions A, 1987, 18(2): 223–231.
[28] Qui W. Growth and characterization of bismuth tri-iodide single crystals by modified vertical Bridgman method. The United States: University of Florida, 2010, 3436423.
[29] Bi Y J, Abell J S. Microstructural characterization of Terfenol-D crystals prepared by the Czochralski technique. Journal of Crystal Growth, 1997, 172: 440–449.
[30] Li Kai, Hu Wenrui. Effect of non-uniform magnetic field on crystal growth by floating-zone method in microgravity. Science in China (series A), 2001, 44(8):1056–1063.
[31] Mei W, Okane T, Umeda T. Magnetostriction of Tb-Dy-Fe crystals. Journal of Applied Physics, 1998, 84(11): 6208–6216.
[32] Higuchi M, Masubuchi Y, Nakayama S, et al. Single crystal growth and oxide ion conductivity of apatite-type rare-earth silicates. Solid State Ionics, 2004, 174(1–4): 73–80.
[33] Xie J W, Fort D, Bi Y J, et al. Microstructure and magnetostrictive properties of Tb-Dy-Fe (Al) alloys. Journal of Applied Physics, 2000, 87(9): 6295–6297.
[34] Reinhard U. The historical development of the Czochralski method. Journal of Crystal Growth, 2014, 401: 7–24.
[35] Clark A E, Verhoven J D, McMasters O D, et al. Magnetostriction in twinned [112] crystals of $Tb_{0.27}Dy_{0.73}Fe_2$. IEEE Transactions on Magnetics, 1986, 22(5): 973–975.
[36] Hu Yong, Ding Yu-tian, Wang Xiao-li, et al. Heat treatment technology of <110> oriented TbDyFe alloy. Transactions of Materials and Heat Treatment, 2012, 33(11): 6–11.
[37] Wu W, Tang H, Zhang M, et al. Effect of heat treatment on the mechanical properties of<110> oriented TbDyFe giant magnetostrictive material. Journal of Alloys and Compounds, 2006, 413(1): 96–100.
[38] Wang Bowen, Cao Shuying, Huang Wenmei. Magnetostrictive materials and devices. Metallurgical Industry Press, 2008, 070625: 122. (in Chinese)
[39] Li Kuo-she, Xu Jing, Yang Hong-chuan, et al. Development of Rare Earth Giant Magnetostrictive Materials. Chinese Rare Earths, 2004, 25(4): 51–56.
[40] Zeng F, Lou J J, Zhu S J. Study on Giant Magnetostrictive Material with Design and Simulation of Displacement Magnifying Mechanism. Advanced Materials Research, 2013, 675: 219–226.
[41] Srisukhumbowornchai N, Guruswamy S. Large magnetostriction in directionally solidified FeGa and FeGaAl alloys. Journal of Applied Physics, 2001, 90(11): 5680–5688.
[42] Yin H Y, Liu J J, Pan Z B, et al. Magnetostriction of $Tb_xDy_{0.9-x}Nd_{0.1}(Fe_{0.8}Co_{0.2})_{1.93}$ compounds and their composites ($0.20 \leqslant x \leqslant 0.60$). Journal of Alloys and Compounds, 2014, 582: 583–587.
[43] Restorff J B, Wun-Fogle M, Clark A E. Temperature and stress dependences of the magnetostriction in ternary and quaternary Terfenol alloys. Journal of Applied Physics, 2000, 87(9): 5786–5788.
[44] Wang B, Lv Y, Li G, et al. The magnetostriction and its ratio to hysteresis for Tb-Dy-Ho-Fe alloys. Journal of Applied Physics, 2014, 115(17): 902–904.
[45] Busbridge S C, Piercy A R. Mannetomechanical properties and anisotropy compensation in quaternary rare earth-iron materials of the type $Tb_xDy_yHo_zFe_2$. IEEE Transactions on Magnetics, 1995, 31(6): 4044–4046.
[46] Guo Z J, Busbridge S C, Zhang Z D, et al. Microstructure, magnetic properties, and spontaneous magnetostriction of $Tb_{0.2}Pr_{0.8}(Fe_{0.4}Co_{0.6})_x$. IEEE Transactions on Magnetics, 2000, 36(5): 3217–3218.
[47] Wang B W. Microstructure and magnetostriction of $(Dy_{0.7}Tb_{0.3})_{1-x}Pr_xFe_{1.85}$ and $(Dy_{0.7}Tb_{0.3})_{0.7}Pr_{0.3}Fe_y$ alloys. Applied Physics Letters, 1996, 69(22): 3429–3431.
[48] Tang Y M, Chen L Y, Zhang L, et al. Temperature dependence of the magnetostriction in polycrystalline $PrFe_{1.9}$ and $TbFe_2$ alloys: Experiment and theory. Journal of Applied Physics, 2014, 115(17): 173902.
[49] Yin Hongyun, Liu Jinjun. Research Progress of $MgCu_2$-Type Giant Magnetostrictive Materials with Pr. Rare Metal Materials and Engineering, 2014, 43(5): 1275–1280.
[50] Ren W J, Zhang Z D, Zhao X G. Magnetostriction and anisotropy compensation in $Tb_xDy_{1-x}Pr_{0.3}(Fe_{0.9}B_{0.1})_{1.93}$ alloys. Applied Physics Letters, 2004, 84(4): 562–564.
[51] Ren W J, Zhang Z D, Song X P, et al. Composition anisotropy compensation and spontaneous magnetostriction in $Tb_{0.2}Dy_{0.8-x}Pr_x(Fe_{0.9}B_{0.1})_{1.93}$ alloys. Applied Physics Letters, 2003, 82(16): 2664–2666.
[52] Ren W J, Liu J J, Li D, et al. Direct experimental evidence for anisotropy compensation between Dy^{3+} and Pr^{3+} ions. Applied Physics Letters, 2006, 89(12): 122506.
[53] Pan Z B, Liu J J, Liu X Y, et al. Structural, magnetic and magnetoelastic properties of Laves-phase $Tb_{0.3}Dy_{0.6}Nd_{0.1}(Fe_{1-x}Co_x)_{1.93}$ compounds ($0 \leqslant x \leqslant 0.40$). Intermetallics, 2015, B64: 1–5.
[54] Lihong Xu, Chengbao Jiang, Chungen Zhou, et al. Magnetostriction and corrosion resistance of $Tb_{0.3}Dy_{0.7}(Fe_{1-x}Si_x)_{1.95}$ alloys. Journal of Alloys and Compounds, 2008, 455(1–2): 203–206.
[55] Wei Wu, Maocai Zhang, Xuexu Gao, et al. Effect of two-steps heat treatment on the mechanical properties and magnetostriction of <110> oriented TbDyFe giant magnetostrictive material. Journal of Alloys and Compounds, 2006, 416: 256–260.
[56] Chengbao Jiang, Yan Zhao, Lihong Xu, et al. Orientation, morphology and magnetostriction of a heat-treated <110> oriented TbDyFe alloy. Journal of Alloys and Compounds, 2004, 373: 167–170.
[57] Jiang C, Zhao Y, Xu L, et al. Orientation, morphology and magnetostriction of a heat-treated<110> oriented TbDyFe alloy. Journal of Alloys and Compounds, 2004, 373(1): 167–170.
[58] Wang Bo-wen, Yan Rong-ge. Rare-earth Giant Magnetostrictive Materials, Application and Devices. Journal of Hebei University of Technology, 2004, 33(2): 16–22.
[59] Jia Z Y, Liu H F, Wang F J, et al. Research on a novel force sensor based on giant magnetostrictive material and its model.

Journal of Alloys and Compounds, 2011, 509(5): 1760–1767.
[60] Olabi A G, Grunwald A. Design and application of magnetostrictive materials. Materials & Design, 2008, 29(2): 469–483.
[61] Joseph M K, Yutang D, Xian Z, et al. Femtosecond Laser Ablated FBG Multitrenches for Magnetic Field Sensor Application. IEEE Photonics Technology Letters, 2015, 27 (16):1717–1720.
[62] Kubo E, Haibara T, Mori Y, et al. Ultrasonic cleaning method and ultrasonic cleaning apparatus: U.S. Patent Application 13/892, 327, 2013-5-13.
[63] Niemczewski B. Observations of water cavitation intensity under practical ultrasonic cleaning conditions. Ultrasonics Sonochemistry, 2007, 14(1): 13–18.
[64] Kwan J J, Graham S, Myers R, et al. Ultrasound-induced inertial cavitation from gas-stabilizing nanoparticles. Physical Review E, 2015, 92(2): 023019.
[65] Eskin G I, Eskin D G. Ultrasonic treatment of light alloy melts. CRC Press, 2014: 32–44.
[66] Mazue G, Viennet R, Hihn J Y, et al. Large-scale ultrasonic cleaning system: Design of a multi-transducer device for boat cleaning (20 kHz). Ultrasonics Sonochemistry, 2011, 18(4): 895–900.
[67] Zhimei M. Research Progress in Ultrasonic Scale Inhibition and Elimination. Sino-Global Energy, 2008, 13(4): 92–96. (In Chinese)
[68] Bhosale S B, Pawade R S, Brahmankar P K. Effect of process parameters on MRR, TWR and surface topography in ultrasonic machining of alumina–zirconia ceramic composite. Ceramics International, 2014, 40(8): 12831–12836.
[69] Liu D F, Cong W L, Pei Z J, et al. A cutting force model for rotary ultrasonic machining of brittle materials. International Journal of Machine Tools and Manufacture, 2012, 52(1): 77–84.
[70] Panteli A, Robson J D, Brough I, et al. The effect of high strain rate deformation on intermetallic reaction during ultrasonic welding aluminium to magnesium. Materials Science and Engineering: A, 2012, 556: 31–42.
[71] Panteli A, Chen Y C, Strong D, et al. Optimization of aluminium-to-magnesium ultrasonic spot welding. JOM, 2012, 64(3): 414–420.
[72] Watanabe T, Sakuyama H, Yanagisawa A. Ultrasonic welding between mild steel sheet and Al-Mg alloy sheet. Journal of Materials Processing Technology, 2009, 209(15): 5475–5480.
[73] Matsuoka S, Imai H. Direct welding of different metals used ultrasonic vibration. Journal of Materials Processing Technology, 2009, 209(2): 954–960.
[74] Matsuoka S. Ultrasonic welding of ceramics/metals using inserts. Journal of Materials Processing Technology, 1998, 75(1): 259–265.
[75] Mason T J. Therapeutic ultrasound an overview. Ultrasonics Sonochemistry, 2011, 18(4): 847–852.
[76] Inoue K, Nakane Y, Michiura T, et al. Ultrasonic scalpel for gastric cancer surgery: a prospective randomized study. Journal of Gastrointestinal Surgery, 2012, 16(10): 1840–1846.
[77] Wang Z, Xu Y, Suman B. Research status and development trend of ultrasonic oil production technique in China. Ultrasonics Sonochemistry, 2015, 26: 1–8.
[78] Chen T C, Shen Y H, Lee W J, et al. An economic analysis of the continuous ultrasound-assisted oxidative desulfurization process applied to oil recovered from waste tires. Journal of Cleaner Production, 2013, 39: 129–136.
[79] Adhikari B, De D, Maiti S. Reclamation and recycling of waste rubber. Progress in Polymer Science, 2000, 25(7): 909–948.
[80] Wan M W, Yen T F. Enhance efficiency of tetraoctylammonium fluoride applied to ultrasound-assisted oxidative desulfurization (UAOD) process. Applied Catalysis A: General, 2007, 319: 237–245.
[81] Quek A, Balasubramanian R. Liquefaction of waste tires by pyrolysis for oil and chemicals-a review. Journal of Analytical and Applied Pyrolysis, 2013, 101: 1–16.
[82] Holst O, Stenberg B, Christiansson M. Biotechnological possibilities for waste tyre-rubber treatment. Biodegradation, 1998, 9(3–4): 301–310.
[83] Al-Lal A M, Bolonio D, Llamas A, et al. Desulfurization of pyrolysis fuels obtained from waste: Lube oils, tires and plastics. Fuel, 2015, 150: 208–216.
[84] Liu L, Wen J, Yang Y, et al. Ultrasound field distribution and ultrasonic oxidation desulfurization efficiency. Ultrasonics Sonochemistry, 2013, 20(2): 696–702.
[85] Chen T C, Shen Y H, Lee W J, et al. The study of ultrasound-assisted oxidative desulfurization process applied to the utilization of pyrolysis oil from waste tires. Journal of Cleaner Production, 2010, 18(18): 1850–1858.
[86] Wan M W, Yen T F. Portable continuous ultrasound-assisted oxidative desulfurization unit for marine gas oil. Energy & Fuels, 2008, 22(2): 1130–1135.
[87] Yao Xiu-qing, Zhang Jie, Li Fei-fei, et al. Recent Process of Desulfurization Technology of the Clean Fuel. Journal of Liaoning University of Petrol EUM and Chemical Technology, 2004, 24(1): 39–42.1
[88] Dong Chengchun. A brief introduction of ultrasonic desulfurization. Rubber & Plastics Resources Utilization, 2012(3): 27–29. (In Chinese)